

HENRY

Hydraulic Engineering Repository

Ein Service der Bundesanstalt für Wasserbau

Conference Paper, Published Version

Koll, Klaus; Koll, Katinka; Dittrich, Andreas

Sediment transport over static armour layers and its impact on bed stability

Verfügbar unter/Available at: <https://hdl.handle.net/20.500.11970/99736>

Vorgeschlagene Zitierweise/Suggested citation:

Koll, Klaus; Koll, Katinka; Dittrich, Andreas (2010): Sediment transport over static armour layers and its impact on bed stability. In: Dittrich, Andreas; Koll, Katinka; Aberle, Jochen; Geisenhainer, Peter (Hg.): River Flow 2010. Karlsruhe: Bundesanstalt für Wasserbau. S. 929-936.

Standardnutzungsbedingungen/Terms of Use:

Die Dokumente in HENRY stehen unter der Creative Commons Lizenz CC BY 4.0, sofern keine abweichenden Nutzungsbedingungen getroffen wurden. Damit ist sowohl die kommerzielle Nutzung als auch das Teilen, die Weiterbearbeitung und Speicherung erlaubt. Das Verwenden und das Bearbeiten stehen unter der Bedingung der Namensnennung. Im Einzelfall kann eine restriktivere Lizenz gelten; dann gelten abweichend von den obigen Nutzungsbedingungen die in der dort genannten Lizenz gewährten Nutzungsrechte.

Documents in HENRY are made available under the Creative Commons License CC BY 4.0, if no other license is applicable. Under CC BY 4.0 commercial use and sharing, remixing, transforming, and building upon the material of the work is permitted. In some cases a different, more restrictive license may apply; if applicable the terms of the restrictive license will be binding.



Sediment transport over static armour layers and its impact on bed stability

Klaus Koll, Katinka Koll & Andreas Dittrich

Leichtweiß-Institut für Wasserbau, TU Braunschweig, Braunschweig, Germany

ABSTRACT: The bed surface of gravel bed rivers is typically stabilized by static armour layers, which develop under limited sediment supply conditions. However, investigations of bed stability mainly focused on clear water flow conditions, and only few studies on the effect of bed load transport on the stability of static armour layers are reported. First results of laboratory experiments carried out to investigate this topic as well as the influence of an armour layer on transport processes are reported in this paper. Tracer experiments were carried out in a 20 m long, 0.5 m wide and 0.6 m high tilting flume in the hydraulic laboratory of the Leichtweiß-Institut für Wasserbau, Technische Universität Braunschweig, Germany. The layer of bed material consisting of a sand-gravel mixture with grain sizes between 0.7 mm and 55 mm had an initial height of 20 cm. After an armour layer was fully developed, i.e. when the transport rate for a specific flow was negligible, coloured sediment was placed on top of the surface. The tracer bar had a height of 2.5 cm, a length of 25 cm and a width of 50 cm. The added sediment consisted of fractions in the range from sand to gravel. A discharge was adjusted higher than the critical discharge of the tracer but lower than the one of the static armour layer. The transport behaviour of the tracer as well as its impact on the bed stability was investigated. Transport distances and velocities increase with increasing relative shear stress and thus with decreasing grain size of the tracer. The transport velocities decrease with run time. Also the response of the armour layer measured by transport rates of eroded bed material depends on the relative shear stress. The transport rate tends to increase with increasing relative shear stress although the amount of eroded bed material is small.

Keywords: Tracer experiments, Sediment transport, Armour layer, Bed stability

1 INTRODUCTION

An important aim of gravel bed river restoration is initiating and supporting a dynamic river bed with, e.g., reforming gravel bars, pools, riffles, etc. The absence of these morphological structures is mainly due to a limited amount of sediment available for being transported. Moreover, the bed surfaces are characterized by static armour layers, which develop under limited sediment supply conditions.

Sediment supply can be enhanced by, e.g., removal of bank protection or deposition of additional sediment on the river bed. However, the additional sediment is often finer than the bed surface material and well mixed. Thus, the critical shear stress of the additional sediment is lower than the critical shear stress of the armour layer and the material can be transported while the river bed is still stable.

Prediction of the morphological development as well as assessment of risks during flood events requires knowledge of dispersion of the additional sediment, transport distance and velocity, and of the response of the existing river bed.

Investigations of the influence of transported sediment on the stability of a static armour layer reported mobilisation of bed material which is immobile under clear water flow conditions (Jackson & Beschta 1984, Hassan & Church 2000, Koll 2002, 2004). Jackson & Beschta (1984) and Hassan & Church (2000) added sediment which was much finer than the bed material and concluded that the erosion is caused by a reduced characteristic diameter of the surface material.

According to Koll (2002, 2004) the transport rates of bed material were highest at the beginning of a feeding experiment, i.e. the amount of eroded bed material reduced with ongoing feeding duration. Thus, the erosion of bed material cannot be

attributed to a change of the characteristic diameter but to the adaptation of the flow field on changed boundary conditions given by the movement and deposition of particles. The transport processes depended on feeding duration and a combination of feeding rate and grain size of the feeding material. However, a mountain river with a distinct step-pool system was simulated in the experiments. Further experiments are required to check if the results can be transferred to gravel bed rivers with milder slopes, which is one aim of the experiments presented here.

A second aim is to investigate the distribution, transport distance and velocity of tracer transported over an armour layer while the bed would remain stable under clear water flow conditions. To the knowledge of the authors no such experiments are published.

Tracer experiments carried out in gravel bed rivers showed that the travel velocity increases with increasing shear stress and decreasing grain size (e.g., Ferguson et al. 2002, Faulhaber & Riehl 2000, Gözl & Trompeter 2000). The dimensionless advective velocity of tracer u_G^* is defined as

$$u_G^* = \frac{u_{Ti}}{\sqrt{\frac{\rho_s - \rho}{\rho} \cdot g \cdot d_{Ti}}} \quad (1)$$

with u_{Ti} [m/s] advective velocity of the tracer with grain size d_{Ti} [mm] using the balance point of the tracer distribution, g [m/s²] gravity acceleration, ρ_s [kg/m³] sediment density, ρ [kg/m³] water density.

Ferguson et al. (2002) conducted field measurements with tracer pebbles with a large time scale during several years. They developed a formula (Eq. 2) to calculate the dimensionless transport velocity considering the grain size of the bed surface

$$u_G^* = \frac{u_{Ti}}{\sqrt{g \cdot d_{Ti}}} = a \cdot \tau^{*b} \cdot e^{(c \cdot d_{Ti} / d_{50})} \quad (2)$$

with $\tau^* = \tau_0 / [(\rho_s - \rho) \cdot g \cdot d_{50}]$ [-] dimensionless bed shear stress, d_{50} [mm] characteristic diameter of the bed material, $\tau_0 = \rho \cdot g \cdot h \cdot I$ [N/m²] bed shear stress, h [m] water depth, I [-] slope.

The coefficients a , b , and c depend on the duration between two surveys. The tracer were placed in 1991 and the dispersion was analysed after 2 years in 1993, and after another 6 years in 1999. The long-term transport velocity decreased significantly independent of the grain size of the tracer, partly due to the fact that the tracer were buried. The slowdown of the tracer was also observed by Faulhaber & Riehl (2000) and Gözl &

Trompeter (2000) who studied tracer transport in the River Elbe and the River Rhine, respectively. Gözl & Trompeter (2000) observed that the velocity of the tracer front was twice as high as the velocity of the balance point. However, transport events of the tracer material were not distinguished from transport events of the river bed.

Laboratory investigations concentrated also mainly on flow situations where the tracer were transported together with the bed material. For instance Wong et al. (2007) investigated the transport of well sorted gravel under equilibrium transport conditions in laboratory experiments. As they did not vary the grain size of the tracer the resulting equation to calculate the dimensionless advective transport velocity (Eq. 3) is only a function of the dimensionless bed shear stress.

$$u_G^* = 1.67 \cdot (\tau^* - 0.0549)^{0.9} \quad (3)$$

Promny (2008a, b) studied the transport processes of tracer over a flat bed as well as during the presence of bed forms. Due to the dunes the tracer particles moved faster than in case of a flat bed. In contrast to the results of field experiments a dependency of the grain size on the transport velocity was not observed. Promny (2008a, b) hypothesized that the lower velocity of coarser grains in rivers is caused by higher burial rates and deeper burial depths which could not be observed in the flume experiments because of the limited depth of the sediment layer.

This paper introduces tracer experiments carried out to improve the understanding of the physics of transport processes over static armour layers and to examine the influence of bed load on armour layer stability. Different stabilities of tracer and bed material are considered by varying the grain size of the tracer and the discharge during the experiment. First results of tracer travel distance and velocity and of eroded bed material are presented.

2 EXPERIMENTS

2.1 Setup

The experiments were carried out in a 0.9 m wide, 0.6 m high, and 20 m long tilting flume in the laboratory of the Leichtweiß-Institute for Hydraulic Engineering. The slope of the flume was adjusted to 5 ‰. Over a length of 17.3 m the width was reduced to 0.5 m. The last 2.7 m of the flume were used to collect eroded sediment in a removable sediment trap. The discharge was adjusted with a valve at the inlet and measured with an Inductive Flow Meter (IDM) with an accuracy of

± 0.05 l/s. Uniform flow conditions were adjusted by a weir at the end of the flume.

A well mixed coarse sediment mixture ($0.7 \text{ mm} < d < 55 \text{ mm}$, $d_m = 8.3 \text{ mm}$) was placed in the flume with a height of 0.2 m . The sediment body was stabilized at the downstream end with a 20 cm high sill made of perforated metal to enable flow in the subsurface layer. The upstream end was stabilized by a 1 m long layer of coarse gravel to limit scouring of the bed downstream of the flow straightener.

In first experiments the critical discharge of the armour layer with maximum bed stability was determined. Maximum bed stability means that the bed stabilizes itself without a significant change of the bed slope. A higher discharge would result in a reduction of the bed slope or the transport rate would not fall below the value which defines negligible bed load transport. The threshold of negligible transport was defined to $400 \text{ g}/(\text{m}\cdot\text{h})$. Close to the end of the armouring process the sediment trap was emptied every hour in order to determine the transport rate per hour. The armour layer was defined as being developed if the threshold value was not exceeded for eight subsequent measurements. The critical discharge Q_{cmax} for the combination of subsurface material and bed slope was determined to 130 l/s which corresponds to a critical shear stress $\tau_{cmax} = 12.6 \text{ N}/\text{m}^2$.

The development of an armour layer takes about 400 hours. In order to avoid its complete destruction due to the transport of the tracer material, the tracer experiments presented here were carried out with an intermediate armour layer developed by adjusting $Q_c = 100 \text{ l/s}$ ($\tau_c = 10.7 \text{ N}/\text{m}^2$). The sieve curves of the initial material Ax, of the intermediate armour layer Zx, and of the armour layer with maximum bed stability Dx are shown in Figure 1.

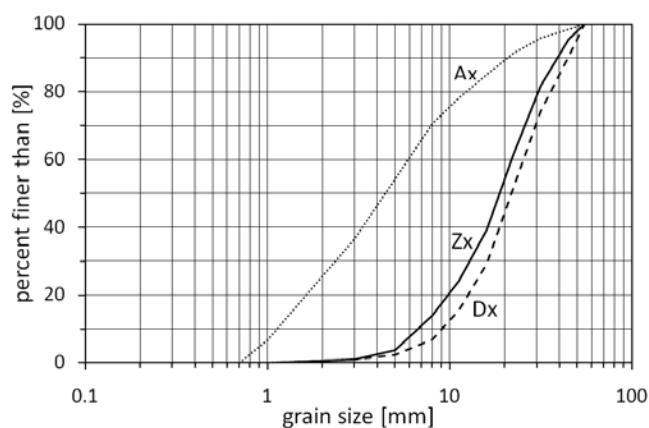


Figure 1. Sieve curves of the initial material Ax (dotted line), the intermediate armour layer Zx (solid line), and the armour layer with maximum bed stability Dx (dashed line).

2.2 Experimental procedure

After the armour layer was developed, the grain size distribution of the bed surface was determined by analysing orthogonal pictures and applying the line-by-number method of Fehr (1987). The bed slope was measured by geometrically correct levelling over the length of the gravel bed with a distance of 10 cm between the measuring points (accuracy $\pm 0.5 \text{ mm}$). The experimental discharge Q_{exp} was adjusted and was held constant for 5 hours to determine the basic transport rate of bed material g_0 .

The flume was dried and the coloured tracer material was deposited on top of the armour layer (see section 2.3). The flume was slowly filled with water to avoid erosion of the sediment during readjustment of Q_{exp} . The discharge and the predetermined weir position for uniform flow conditions were adjusted simultaneously.

During the experiments discharge, water level, sediment output and tracer distribution were determined. The water level was measured every 30 min by using the method of corresponding water levels with an accuracy of $\pm 0.1 \text{ mm}$. 10 measuring positions were located with a distance of 1.5 m starting 2.5 m downstream of the flume inlet.

The amount and grain size distribution of eroded sediment was determined by periodic exchange of the bed load trap. The time steps were two times 15 min and afterwards 30 min until the end of the experiment. The experiments continued until no significant movement of the tracer material was observed visually. Due to the painted tracer it was possible to distinguish between eroded bed material and tracer.

For the observation of the time dependent tracer distribution the discharge was stopped periodically and orthogonal photos of the bed were taken. The photos were analysed by using computer aided image analysis. At the end of an experiment the bed was subdivided in cells of 10 cm by 10 cm . The tracer material was collected manually and the amount was determined by weighing. The results of the manually determined tracer distribution are used to calibrate the image analysis. The comparison between image analysis and measurement is exemplarily shown for run E2 in Figure 2. The shape of the tracer distribution can be determined by image analysis with a high accuracy (deviation less than 1%). Also the determination of the amount of tracer depending on the position along the flume gives good results. However, the amount is underestimated by image analysis if the tracer is not single layer distributed. Additional experiments for calibration are planned to improve the results of the methodology.

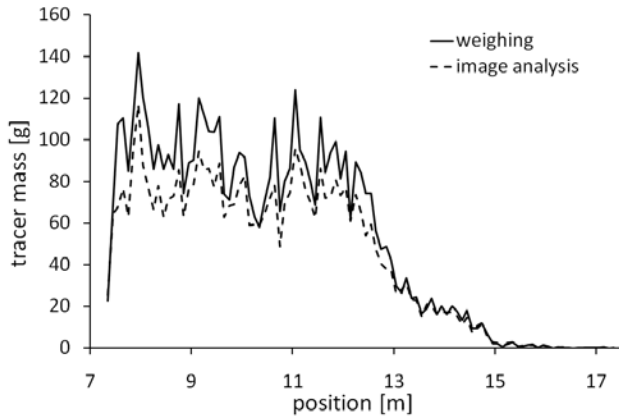


Figure 2. Comparison of measured and image analysed longitudinal tracer distribution for run E2 ($d_T = 5-8$ mm).

2.3 Tracer experiments

The experiments were carried out to study the distribution of sediment which is deposited in a river to initiate morphological processes as well as the impact of this sediment on the existing river bed. Thus, the tracer material was placed on top of the armour layer (see Figure 3) instead of feeding it.

The bar had a height of 0.025 m, a length of 0.25 m, and a width of 0.5 m. The height of the bar was limited in order to minimize bed erosion caused by the geometry of the bar. The upstream end of the bar was located 7.375 m downstream of the flume inlet. Thus, a 9.675 m long section was available to investigate the transport of the tracer as well as the response of the armour layer.

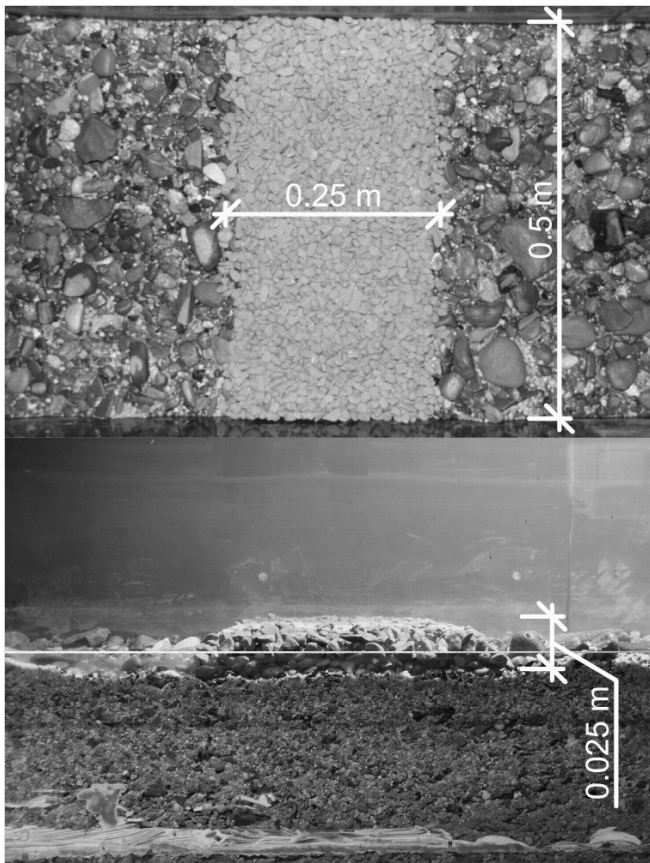


Figure 3. Deposition of the tracer material.

The tracer material was coloured to distinguish between bed and tracer material. So far, five experiments were carried out with four different grain sizes of the tracer material and two different discharges Q_{exp} during the experiment. The experiments are summarized in Table 1.

Each experiment started with adjusting a discharge of 80 l/s, i.e. a discharge lower than the critical discharge of the armour layer. In three experiments the discharge was kept constant until the end ($Q_{exp} = 80$ l/s). In two experiments after 15 min the discharge was increased to the critical discharge of the armour layer, i.e. $Q_{exp} = 100$ l/s. The ratio of the critical shear stress of the tracer τ_{cT} and the shear stress of the flow τ_0 ranged between 1.04 and 3.10 (see Table 1).

In experiments E3 and E5 the critical discharge of the tracer material was only slightly exceeded by τ_0 resulting in durations of only 210 min. The duration of the other experiments was $T_{end} = 930$ min.

Table 1. Parameters of tracer experiments

(Q_{exp} = discharge during experiment, τ_0 = shear stress of flow, d_T = grain size of tracer, τ_{cT} = critical shear stress of tracer, T_{end} = duration of experiment)

Run	Q_{exp} [l/s]	τ_0 [N/m ²]	d_T [mm]	τ_{cT} [N/m ²]	τ_0/τ_{cT} [-]	T_{end} [min]
E1	80	9.3	3-5	3.0	3.10	930
E2	80	9.3	5-8	5.0	1.86	930
E3	80	9.3	8-11	7.2	1.29	210
E4	100	10.7	8-11	7.2	1.49	930
E5	100	10.7	11-16	10.3	1.04	210

3 RESULTS

Results of transport distances and tracer velocities depending on the tracer grain size, the applied bed shear stress, and the run time as well as the impact of tracer transport on bed stability are presented and discussed.

3.1 Transport distance and velocity

The percentage of the area of the bed surface covered by tracer was determined for each time step by image analysis of the orthogonal photos. In Figure 4 the longitudinal distribution of the tracer is exemplarily shown for run E1 at the time steps 30, 210 and 930 min. The widening and flattening of the tracer distribution with run time as well as the progression of the tracer front becomes obvious. Moreover, it can be seen that in run E1 the tracer front already reached the end of the gravel bed at $T_{end} = 930$ min.

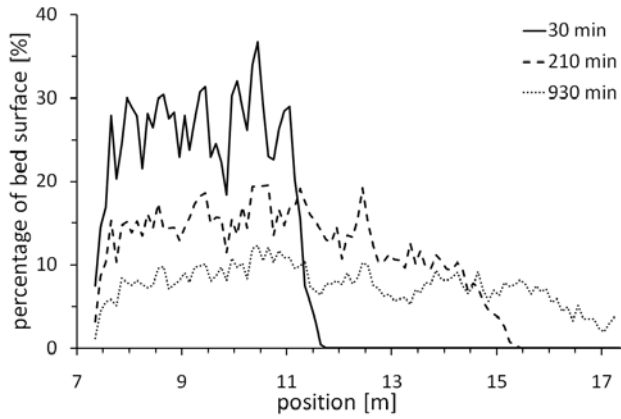


Figure 4. Longitudinal distribution of tracer for run E1 ($d_T = 3 - 5$ mm) at run time $T = 30, 210$ and 930 min.

The transport distance of the front L_F and the mean transport distance L_S were determined for each time step. The tracer front is defined as the position which has not been exceeded by 99 % of the tracer (Promny, 2008a). L_S is based on the position of the balance point of the tracer distribution.

The time series of L_S for runs E1 - E5 (see Table 1) are plotted in Figure 5. The gradient of the curves reduce with time indicating that the advective tracer velocity decreased. Comparing the mean transport distances for runs E1 - E3 the influence of the grain size becomes obvious: L_S increases with decreasing grain size. The effect of the grain size is much less pronounced for runs E4 and E5 which can be attributed to the smaller difference in τ_0/τ_{cT} .

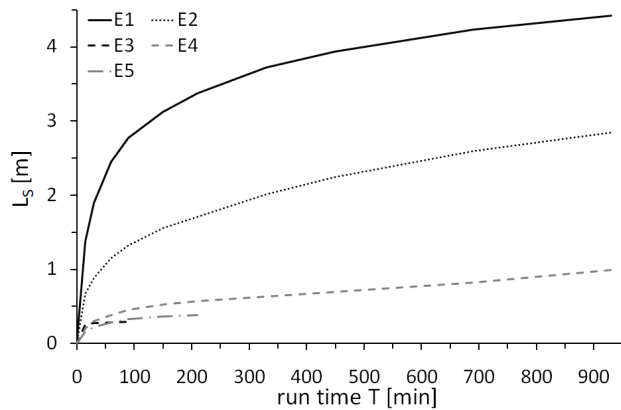


Figure 5. Mean transport distance L_S as a function of run time.

Plotting L_S and L_F as a function of τ_0/τ_{cT} , e.g., for $T = 60$ min (Figure 6) reveals that both transport distances increase with relative shear stress following power functions but with different gradients.

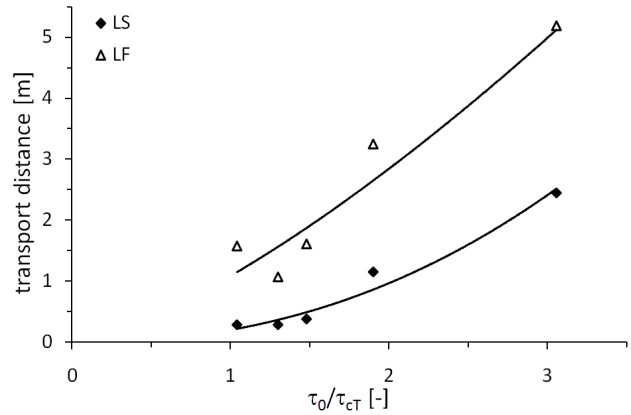


Figure 6. Mean transport distance L_S and transport distance of the tracer front L_F at $T = 60$ min as a function of relative shear stress τ_0/τ_{cT} .

The development of L_F/L_S with run time is plotted in Figure 7. Values above 1 indicate an increasing distance between the front and the balance point of the tracer distribution. The smaller the grain size of the tracer the smaller is the difference between front and mean velocity. Although the travel distance in run E1 was distinctively larger than in run E2 the ratio L_F/L_S is in the same order of magnitude. Thus, the tracer with grain size 3-5 mm and 5-8 mm was distributed in a comparable way.

The magnitude and the shape of the curves for run E3 - E4 deviate from the first two runs. For run E1 and E2 L_F/L_S was almost constant after a run time of 90 min whereas for run E4 and E5 the ratio changed throughout the experiments. It has to be taken into account that the tracer was still transported in run E1 and E2 at $T = 90$ min, but the progression of the tracer was almost negligible after 30 min for run E4 and E5 (see Figure 5).

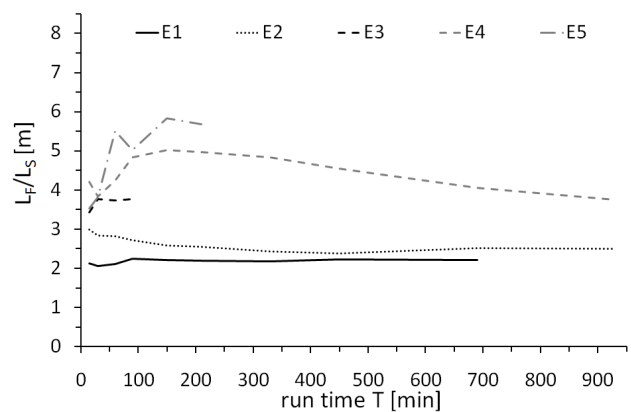


Figure 7. Ratio of the transport distance of the tracer front L_F and the mean transport distance L_S as a function of run time.

The velocity of the tracer front and the advective transport velocity are plotted in a log-log scale in Figure 8 for the runs E1 - E3. For run E1 the velocity of the tracer front at $T = 930$ min could not be calculated, because the tracer front exceeded the end of the gravel bed.

As aforementioned the front velocity is faster than the advective velocity and the velocities decrease with increasing grain size.

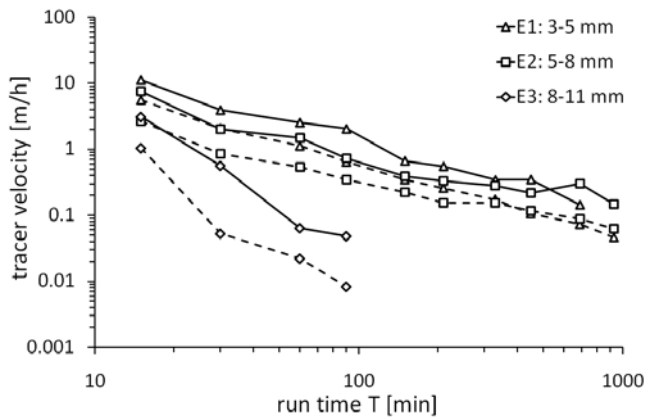


Figure 8. Advective and front velocity for runs E1 - E3 with $Q_{exp} = 80$ l/s (solid line = front velocity; dashed line = advective velocity).

As, e.g., Faulhaber & Riehl (2000) and Ferguson et al. (2002) observed in field studies the transport velocities decreased with increasing run time. However, the slowdown cannot be explained by burial of the tracer as the amount of transported bed material was small (see section 3.2) and thus the percentage of tracer material found in deeper layers of the bed was marginal.

The tracer velocities increased with increasing discharge as can be seen in Figure 9. The velocities of the experiments E3 and E4 with the same tracer grain size but different discharges Q_{exp} are plotted together with run E5. The higher velocities for run E4 compared to E3 are only partly due to the larger relative shear stress τ_0/τ_{cT} . Otherwise tracer transport in run E3 ($\tau_0/\tau_{cT} = 1.29$) would have been faster than in run E5 ($\tau_0/\tau_{cT} = 1.04$). Further experiments are required and planned to explain the differences.

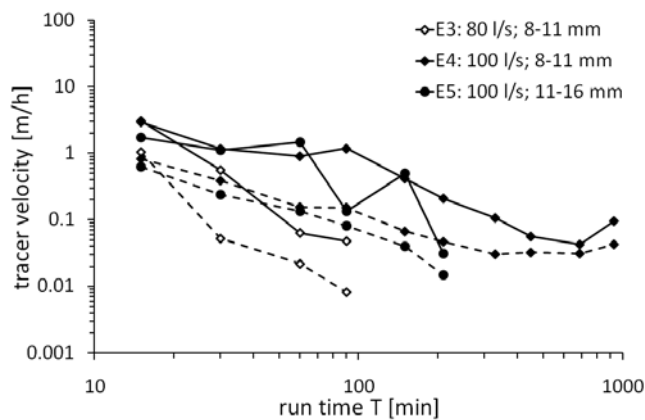


Figure 9. Advective and front velocity for runs E3 - E5 (solid line = front velocity; dashed line = advective velocity).

In order to compare the results to other studies the dimensionless advective velocity u_G^* has been calculated. In the laboratory studies of Promny (2008a, b) and Wong et al. (2007) the tracer mate-

rial was of the same size as the bed material and both, tracer and bed material were transported. In the field study of Ferguson et al. (2002) the tracer material represented fractions of the bed material and the bed surface was in movement, too.

Figure 10 shows the comparison of u_G^* calculated with Eq. (1) for the time span $T = 0-90$ min as well as calculated with Eq. (2) and (3) from Ferguson et al. (2002) and Wong et al. (2007), respectively. Ferguson et al. (2002) did not consider the submerged specific gravity of the sediment. For comparison Eq. (2) was therefore multiplied with the term $((\rho_s - \rho)/\rho)^{-1}$. The parameters of the equation were set to $a = 0.0075$, $b = 0.85$ and $c = -1.25$ according to the short term relation given by Ferguson et al. (2002). As Ferguson et al. (2002) distinguished between tracer and bed material Eq. (2) was used to calculate u_G^* for the smallest and the largest grain size of tracer material used in this study. Moreover, the data of Promny (2008b) are included in Figure 10.

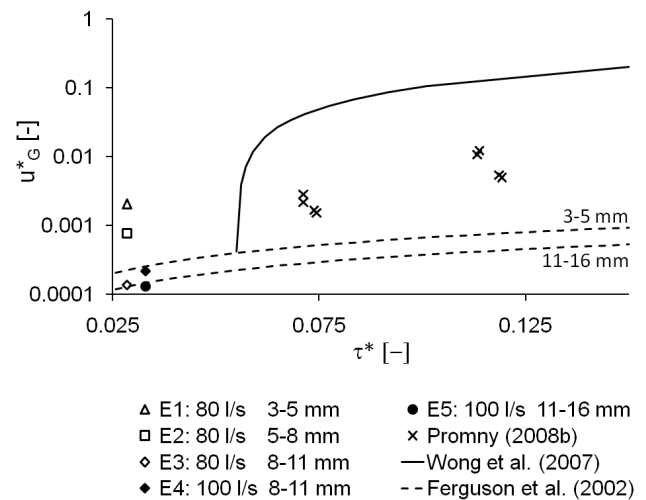


Figure 10. Dimensionless advective velocity u_G^* calculated for $T = 0-90$ min as a function of the dimensionless bed shear stress τ^* .

The relation of Wong et al. 2007 is not valid for $\tau^* < 0.0549$, hence it cannot be applied for the experiments in this research. The velocities of grain sizes 8-11 mm and 11-16 mm are well represented by the equation of Ferguson et al. (2002). However, it has to be considered that the tracer velocity strongly depends on run time and thus u_G^* changes with the time scale.

3.2 Bed stability

The influence of bed load transport on the stability of the armour layer can be assessed by analysing the amount of eroded bed material collected in the sediment trap. The ratio of the transport rate of bed material eroded during the experiments, g_e , and the basic transport rate g_0 (determined during five hours of constant discharge before placing the

tracer, see Section 2.2) is plotted as a function of run time for experiments with $Q_{exp} = 80$ l/s in Figure 11 and with $Q_{exp} = 100$ l/s in Figure 12. The basic transport rates g_0 were determined to 40 g/(m·h) and 210 g/(m·h), respectively.

Throughout the experiments the transport rates of bed material were low, however, exceeded the basic transport rate up to almost 9 times. The fluctuation of eroded bed material is more pronounced for the experiments with smaller sized tracer material and higher relative shear stresses (runs E1 and E2) than for runs E3 - E5. After a certain run time the transport rate of bed material decreased abruptly and remained in the order of magnitude of the basic transport rate until the end of the experiments. It is reasonable to assume that the transport of bed material is related to the transport velocity of the tracer. However, at present this assumption cannot be verified with the available data.

Experiments E3 and E5 were already finished after 210 min due to the definition of the end of an experiment. Besides a negligible progression of the tracer the amount of eroded bed material will be a second criterion for the end of a run in further experiments.

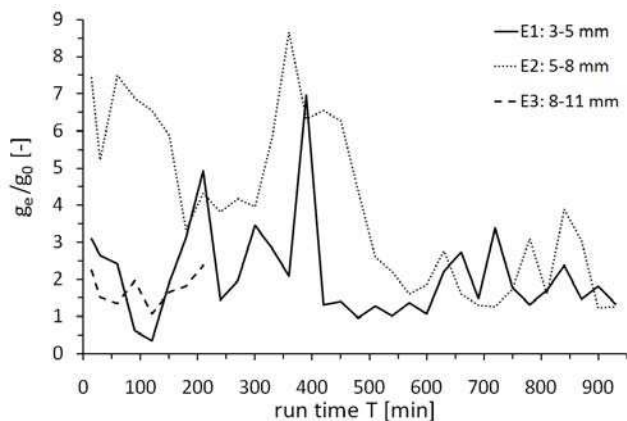


Figure 11. Relative transport rate of eroded bed material g_e/g_0 as a function of run time for experiments with $Q_{exp} = 80$ l/s.

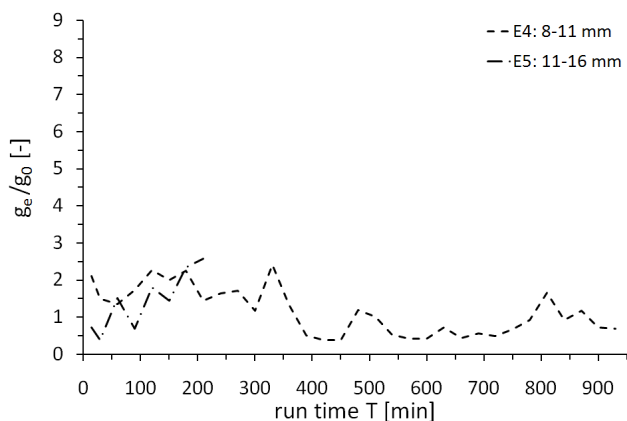


Figure 12. Relative transport rate of eroded bed material g_e/g_0 as a function of run time for experiments with $Q_{exp} = 100$ l/s.

The relative transport rates of bed material were higher for the experiments with the smaller sized tracer material and the higher relative shear stresses (runs E1 and E2). However, the dependency on d_T and τ_0/τ_{cT} is not as clear as for the parameters of the tracer distribution and as reported by Koll (2002, 2004) which becomes more obvious in Figure 13. The relative transport rates of bed material averaged over the period $T = 0$ -210 min are plotted as a function of the ratio of the bed shear stress τ_0 and the critical shear stress of the tracer material τ_{cT} . Regarding the amount of bed material mobilised due to the transported tracer either run E1 or run E2 seems to be an outlier. Further experiments will clarify this result.

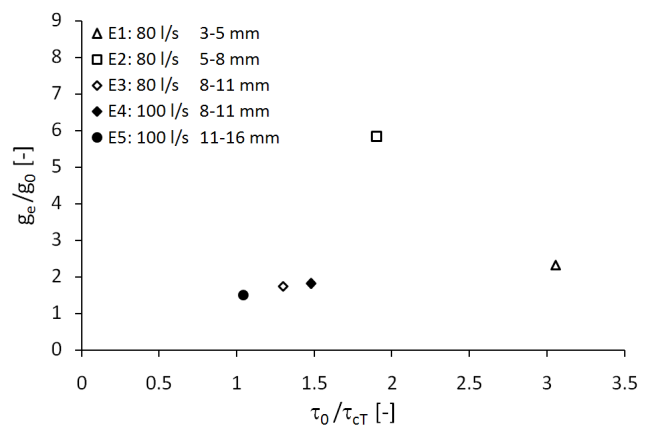


Figure 13. Relative transport rate of eroded bed material g_e/g_0 at $T = 210$ min as function of relative shear stress τ_0/τ_{cT} .

4 CONCLUSION

Preliminary results of tracer experiments are presented. Contrary to published laboratory and field studies this study aims to investigate transport processes of tracer while the bed surface remains stable under clear water flow conditions, i.e. the applied shear stress is lower than the critical shear stress of the bed surface. The knowledge of this processes is required in order to predict the morphological development as well as to assess risks during flood events when reestablish river bed dynamics.

A static armour layer was developed before the tracer was placed on top of it. Five experiments were carried out with four different grain sizes of the tracer material and two discharges. An experiment was finished if the visually observed transport of tracer was negligible.

Transport distances and transport velocities are presented as functions of run time and relative shear stress. Both, the distances and the velocities depend on the relative shear stress and thus on the grain size of the tracer. The higher the difference between applied and critical shear stress the faster the tracer is transported. The transport velocity

decreases with run time. Therefore, it is difficult to compare these results with published data.

Distinguishing between tracer front and balance point of the tracer distribution shows that the front moves faster than the mean tracer mass. The ratio of front and mean transport distance changes with run time. It becomes constant, if the critical shear stress of the tracer is exceeded to a certain factor by the applied shear stress. However, the factor cannot be quantified, yet.

The response of the armour layer on the tracer transport is presented by means of eroded bed material. It can be concluded that bed material is mobilised due to the transport of tracer even if the bed surface is strongly armoured. However, the amount of eroded bed material is small. First results show that the transport rates of bed material depend on the grain size of the tracer, which is in accordance with results of Koll (2002, 2004).

Further experiments are required and planned to improve the results.

ACKNOWLEDGEMENTS

This research is supported by ERDF (European Regional Development Fund) within the INTERREG IVA "Upper Rhine" Programme of the European Union.

REFERENCES

- Faulhaber, P., Riehl, K. 2001. Geschiebezugabe an der Elbe. - BfG-Veranstaltungen 3/2001 Feststoffeintrag, Laufentwicklung und Transportprozesse in schiffbaren Flüssen, Koblenz, Germany, 67-80.
- Fehr, R. 1987. Einfache Bestimmung der Korngrößenverteilung von Geschiebematerial mit Hilfe der Linienzahlanalyse. Schweizer Ingenieur und Architekt 105, 1104-1109.
- Ferguson, R.I., Bloomer, D.J., Hoey, T.B., Werritty, A. 2002. Mobility of river tracer pebbles over different timescales. Water Resour. Res. 38(5), doi:10.1029/2001WR000254, 1045-1052.
- Gölz, E., Trompeter, U. 2001. Transport und Verteilung von Zugabematerial. - Erste Ergebnisse aus den Tracer- Versuchen Iffezheim. - BfG-Veranstaltungen 3/2001 „Feststoffeintrag, Laufentwicklung Koblenz, Germany, 55-65.
- Hassan, M.A., Church, M. 2000. Experiments on surface structure and partial sediment transport on a gravel bed. Water Resour. Res., 36(7), 1885-1895.
- Jackson, W.L., Beschta, R.L. 1984. Influences of increased sand delivery on the morphology of sand and gravel channels. Water Resources Bulletin, 20(4), 527-533.
- Koll, Ka. 2002. Feststofftransport und Geschwindigkeitsverteilung in Raugerinnen. [online], Karlsruhe, Univ., Fak. f. Bauingenieur- und Vermessungswesen, Diss. v. 12.07.2002, <http://www.ubka.uni-karlsruhe.de/cgi-bin/psview?document=2002/bau-verm/12>.

- Koll, Ka. 2004. Transport Processes over Static Armour Layers. Proc. 5th Int. Symp. on Ecohydraulics "Aquatic Habitats: Analysis & Restoration", 12-17 September 2004, Madrid, Spain, Eds. D. Garcia de Jalón Lastra & P.V. Martínez, 442-448.
- Promny, M. 2008a. Advektion und Dispersion von Geschiebe. PhD-Thesis, Institute of Hydrosciences, Bundeswehr University, Munich, Germany.
- Promny, M. 2008b. Propagation velocity of bed load material in dunes. Proc. Int. Conf. on Fluvial Hydraulics River Flow 2008, 3-5 September 2008, Cesme, Turkey. Eds. M. Altinakar, M.A. Kokpinar, I. Aydin, S. Cokgor, and S. Kirkgoz, Kubaba, Izmir, Turkey, Vol. 2, 921-928.
- Wong M., Parker G., DeVries P., Brown T.M., Burges S.J. 2007. Experiments on dispersion of tracer stones under lower-regime plane-bed equilibrium bed load transport, Water Resour. Res. 43, W03440, doi:10.1029/2006WR005172.